Magnetic properties and domain-wall motion in single-crystal $BaFe_{10.2}Sn_{0.74}Co_{0.66}O_{19}$

X. X. Zhang, J. M. Hernàndez, and J. Tejada
Departament de Física Fonamental, Universitat de Barcelona, Diagonal 647, 08028 Barcelona, Spain

R. Solé and X. Ruiz
Laboratori Física Aplicada i Cristallografia. Universitat Rovira i Virgili. 43005 Tarragona, Spain

(Received 10 July 1995; revised manuscript received 26 October 1995)

The magnetic properties of $BaFe_{12}O_{19}$ and $BaFe_{10.2}Sn_{0.74}Co_{0.66}O_{19}$ single crystals have been investigated in the temperature range (1.8 to 320 K) with a varying field from -5 to $+5$ T applied parallel and perpendicular to the c axis. Low-temperature magnetic relaxation, which is ascribed to the domain-wall motion, was performed between 1.8 and 15 K. The relaxation of magnetization exhibits a linear dependence on logarithmic time. The magnetic viscosity extracted from the relaxation data, decreases linearly as temperature goes down, which may correspond to the thermal depinning of domain walls. Below 2.5 K, the viscosity begins to deviate from the linear dependence on temperature, tending to be temperature independent. The near temperature independence of viscosity suggests the existence of quantum tunneling of antiferromagnetic domain wall in this temperature range.

INTRODUCTION

The tunneling effect of magnetization was theoretically predicted by Chudnovsky and Gunther[1] in 1988. Since the pioneering theoretical studies, quantum tunneling of magnetization (QTM), has been a subject of great interests in condensed-matter physics.[2–11] Generally, tunneling in magnets involves two phenomena:[12] (a) tunneling of magnetization in single-domain particles or grains, (in which some 1000 to 10 000 spins rotate together between two different orientations of magnetization), (b) tunneling of domain walls in a film or in bulk magnets; where walls containing $\sim 10^{10}$ spins may tunnel from one pinning center to another.

Most of the experimental studies on QTM are based on the first case, QTM in single-domain particles or grains,[2,3,5,7,8] mostly due to the difficulty in obtaining suitable materials for observing the effect of quantum tunneling of domain walls (QTDW). In our previous work,[13] QTDW was observed in an antiferromagnetic $TbFeO_3$ single crystal in magnetic relaxation measurements. The exponential magnetic relaxation was found in the $TbFeO_3$ single crystal, which corresponds to the existence of a single barrier for the motion of DW. Our present intention is to study the domain-wall motion at low temperatures, using the relaxation measurements, in order to get deeper understanding of the mechanisms involved in domain-wall motion.

Time-dependent effects of magnetization have long been known in magnetic materials: a collection of single-domain ferromagnetic particles, magnetic thin films, and bulk ferromagnetic matters.[2–5,7,8,13] The dynamics of the effects has been assumed to be described by thermally activated processes. For a collection of identical noninteracting single-domain ferromagnetic particles frozen in a nonmagnetic matrix, by applying an external magnetic field, the magnetic moments of the particles can be aligned in one direction. After removing the external field, the magnetic moment decays exponentially with time[14,15]

$$M(t) = M_0 e^{-\Gamma t},$$

$$\Gamma = \Gamma_0 \exp\left(-\frac{U}{k_B T}\right), \tag{1}$$

where M_0 is the remnant magnetic moment just after removing the external field, Γ_0 is the attempt frequency typically taken to be 10^9–10^{11} s^{-1}, k_B is the Boltzmann constant, T is the absolute temperature, $U = KV$ is the height of energy barrier associated with the switching process of magnetic moment of particles and V is the particle volume. The anisotropy constant K is defined by the anisotropy field H_K, and the saturation magnetization M_S as $H_K = 2K/M_S$.

The exponential time dependence of magnetization has been attributed to the single energy barrier height. But such a behavior has never been observed experimentally in particle systems, to our knowledge. Instead, a time dependence of, say, the magnetization follows a logarithmic decay over typically 3–5 decades in time.[3–5,7,8] This nonexponential dependence has been linked to the distribution of energy barrier due to the distribution of size and shape of the particles. Thus, the relaxation of magnetization can be described by[4]

$$M(t) = M_0[1 - S(T)\ln(t)],$$

$$S(T) = \frac{k_B T}{\langle U \rangle}, \tag{2}$$

instead of Eq. (1). Where $S(T)$ is the magnetic viscosity, $\langle U \rangle$ is the average energy barrier over different shapes. The logarithmic time dependence of magnetization has also been observed experimentally in the magnetic thin films and bulk magnetic materials due to the magnetic metastable states in the materials which give a wide distribution of energy barrier heights.[2,4,5,7,8]

Within the frame of a thermally activated process as temperature T decreasing to zero, both the exponential decay rate $\Gamma(T)$ and the magnetic viscosity $S(T)$ goes to zero, that

is, the thermal activation is frozen out.[4] The appearance of nonzero temperature independent of Γ and S below some temperature should be attributed to the nonthermal activation process, i.e., quantum effects.[2–5,7,13]

The barriers associated with the relaxation process are of two types. The intrinsic barriers arising from the magnetic anisotropy contribute to the reversal of magnetization in single-domain particles and nucleation in thin film or bulk materials. The barriers due to the pinning of domain walls are generally attributed to the defects in the materials. Both types of barriers are responsible for the pronounced metastability of magnetic materials, known as hysteresis phenomena.[4]

Hexagonal $BaFe_{12}O_{19}$ is a well-known ferrimagnet with a uniaxial anisotropy lying along the c axis. It has a typical ferrimagnetic structure, with the orientation of magnetic moments of ferric ions in the crystal generally aligned along the c axis. It has been reported [16] that in large single crystals, the domain wall moves freely in response to the change of the external field, i.e., the coercive field $H_C=0$. In order to study the domain-wall motion using the relaxation measurements, we have introduced some substitution of Co and Sn for Fe in the single crystal to produce pinning centers. Clearly the substitution of Co and Sn will change the magnetic properties of $BaFe_{12}O_{19}$ crystal.[17] The effect of the substitution on magnetic properties is interesting for physics and applications.

Here we report the effect of the substitution of Fe by Co and Sn on the magnetic properties of a single crystal of $BaFe_{10.2}Co_{0.66}Sn_{0.74}O_{19}$, and the relaxation study of the domain-wall dynamics.

EXPERIMENTAL

$BaFe_{12}O_{19}$ and $BaFe_{10.2}Sn_{0.74}Co_{0.66}O_{19}$ single crystals were grown from high-temperature solution, by slow cooling using the TSSG (top seeded solution growth) method. A cylindrical vertical furnace with a Pt/Pt 10% Rh control thermocouple and an Eurotherm 818P controller programmer was used in all the growth experiments. Platinum crucibles with a 30 cm^3 volume were used with a solution weight of 40–45 g.

Pure SnO_2 from Merk and Na_2CO_3, B_2O_3, Fe_2O_3, $BaCO_3$, and Co_2O_3 from Merk ''proanalysis'' were used as reagents. The solution composition in the $BaFe_{12}O_{19}$ case was 70 mol % of (0.4 Na_2O-0.6 B_2O_3) and the mol ratio $BaO:Fe_2O_3=1:1.25$. In the case of substituted crystal, the solution composition was 74 mol % of (0.4 Na_2O-0.6 B_2O_3) solvent and the mol ratios $BaO:(Fe_2O_3+CoSnO_3)=1:1.5$ and $Fe_2O_3/CoSnO_3=11:1$. These two compositions have low volatilities, about 0.3 g/day, slight climbing tendencies and low saturation temperatures, 920 and 980 °C, respectively. The axial temperature difference in the each solution was about 30 °C (hot bottom), while the radial one, on the surface, was about 10 °C (hot crucible wall). The solutions were homogenized for 2–4 h at about 50 °C above their saturation temperature. This temperature was accurately determined by dissolving or growing a seed in contact with the solution at temperatures which were close to the saturation one. The growth processes began at temperatures slightly above the accurately determined saturation one (~1 °C) on a seed located in the center of the free surface of the solution. The supersaturation was achieved by slow cooling 20–25 °C at a rate of 0.1–0.5 °C/h. Taking into account the small dimensions of the seed at the beginning of the growth and in order to avoid unstable growth conditions, a slow rotation rate 10 rpm was used in all cases. Finally, the crystals were removed from the solution, cooled to room temperature at a rate of 30–50 °C/h and cleaned with hot diluted nitric acid.

To analyze the incorporation of the different cations in the $BaFe_{12}O_{19}$ crystalline matrix during the growth process, EPMA (electron probe microanalysis) measurements with wavelength dispersive spectroscopy, using a CAMECA Camebax SX 50, were carried out. The results show that the distribution coefficients of the substituting ions do not change appreciably along the different directions of the crystals and the composition for the sample with substitution is $BaFe_{10.2}Sn_{0.74}Co_{0.66}O_{19}$. X-ray analyses of this kind of cobalt- and tin-substituted barium hexaferrites show that Sn^{4+} cations only enter the octahedral sites and a pronounced occupational hierarchy within them is established. That is to say, most of Sn^{4+} cations enter the octahedral $4f_2$ sites and a very small amount of them occupy octahedral $12k$ sites, while they do not enter the octahedral $2a$ sites at all. On the other hand, the Co^{2+} cations are distributed among tetrahedral and octahedral sites with clear preference for tetrahedral $4f_1$ sites. The observed cation site selectivity can be correlated with the uniaxial magnetic anisotropy with an easy direction parallel to the crystallographic c axis.[17]

The magnetic characterization was performed on the $BaFe_{12}O_{19}$ and $BaFe_{10.2}Sn_{0.74}Co_{0.66}O_{19}$ single crystals. The low-field magnetization versus temperature was obtained in the zero-field-cooled and field-cooled processes (ZFC-FC), by which information on the barrier distribution can be obtained. Magnetization versus applied field was performed with applying field to the sample in c axis and perpendicular to the c axis at different temperatures with field varying from −3 to 3 T. Thus, different parameters, like, saturation magnetization M_S, coercive field H_C, and magnetic anisotropy field H_K were obtained.

The relaxation measurements, for studying the dynamic properties of domain-wall motion were performed as follows: first the sample was cooled in an applied field $H_1=10$ Oe to a target temperature, after which the applied field was changed to H_2 (−220 Oe) then the changing of remanent magnetization with time was measured during a few hours. After this measurement, the sample was heated to higher temperature with applied field H_1 and cooled down to another target temperature for next relaxation measurement.

RESULTS AND DISCUSSION

Figure 1 shows the temperature dependence of the dc susceptibility obtained in $BaFe_{12}O_{19}$ and $BaFe_{10.2}Sn_{0.74}Co_{0.66}O_{19}$ single crystals through the ZFC-FC processes. The behavior of the ZFC curve of sample 2 is a typical signature of the domain-wall motion in bulk materials. Comparing the susceptibility data obtained in the ZFC-FC processes, it suggests that the domain walls are obstructed from moving freely by the imperfections of the magnetic structure in the sample as a consequence of the substitution of Co and Sn for Fe. As expected, as the temperature increases in the ZFC process, the domain walls are depinned from the pinning centers by thermal activation. Another fea-

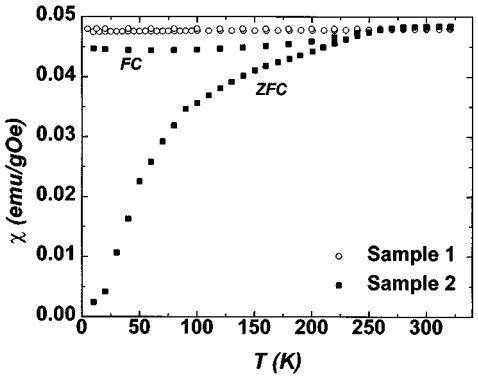

FIG. 1. dc susceptibility obtained in the ZFC-FC process for two samples.

ture should be noted that without the substitution, the ZFC and FC data, obtained in sample 1, almost overlap in the whole experimental temperature range, indicating that domain walls move almost freely in response to a change of applied field (see Fig. 1).

Figure 2 displays the magnetization versus applied field obtained at sample temperature $T=6$ K with the field applied parallel and perpendicular to the c axis for the two samples. From the magnetization data, some characteristic parameters can be obtained, as summarized in Table I. Nonhysteresis behavior in the $M(H)$ data obtained in sample 1 at 6 K for two directions of applied field indicates that due to multidomain behavior, the reversal proceeds almost exclusively by domain-wall motion, and the motion of the walls is not impeded by any crystal imperfections.[16] From the magnetization curves with applied field along and perpendicular to the c axis, it is clearly known that the sample has a perfect uniaxial anisotropy along the c axis; the anisotropy field H_K can be taken where the magnetization curves measured in two directions begin to overlap with each other. From Fig. 1(b), it is known that the easy magnetization direction is along the c axis too. Comparing the magnetization data obtained in two samples with applied field along the c axis, the remarkable difference is that for sample 2, the hysterestic behavior is observed with the coercive field $H_C\sim0.620$ kOe. The saturation of magnetization was observed at $H\sim2.3$ kOe, the same as that in sample 1, indicating that the magnetic structures in two samples are similar. The hysteresis phenomenon in sample 2 suggests that the domain-wall motion is impeded by the pinning centers caused by the substitution. The most interesting features in Fig. 1(b), is the behavior of magnetization curve measured with applied field perpendicular to the c axis. The sharp deviation from the linear dependence of magnetization on applied field at $H\sim2$ kOe and the hysteresis phenomena could be due to the field-induced first-order magnetic transformation.[18] It should be noted that in relatively low fields, the magnetization depends linearly on the applied field (here $0<H<2$ kOe), indicating that in the low-field range, $H<2$ kOe, after the demagnetization state, the anisotropy field is along the c axis. Thus, the anisotropy field can be fitted by the extrapolating of this linear part to the saturation magnetization; $H_K\sim15.97$ kOe was obtained. This extrapolated anisotropy H_K is similar to that obtained in sample 1, which supports the observation that in low fields the magnetic structure in sample 2 is similar to that in sample 1.

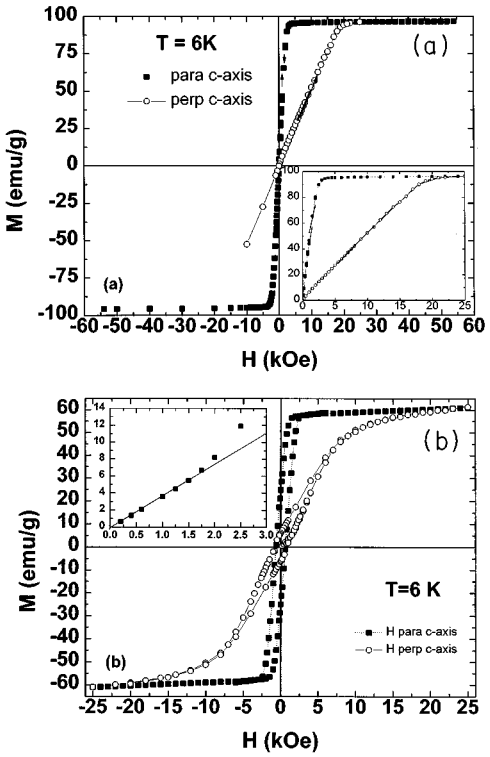

FIG. 2. Magnetization as function of applied field along and perpendicular to the c axis obtained at temperature $T=6$ K. (a) $BaFe_{12}O_{19}$ single crystal, inset: to show the detail of saturation behavior. (b) $BaFe_{10.2}Sn_{0.74}Co_{0.66}O_{19}$ single crystal, Inset show the linear part of $M(H)$ with H applied perpendicular to the c axis.

Magnetic relaxation measurements have been performed in the temperature range 1.9 to 15 K, for studying the domain-wall dynamics, according to the procedure described in the experimental section. The sample was field cooled from 300 K, down to a measuring temperature, after which the field applied to the sample was changed to $H_2=-220$ Oe, then the time dependence of magnetization was mea-

TABLE I. Data of M_S, H_C, H_K, K, χ obtained experimentally.

Sample	M_S (6 K) (emu/g)	M_S (300 K) (emu/g)	$H_{C\parallel}$ (6 K) (kOe)	$H_{C\perp}$ (6 K) (kOe)	H_K (6 K) (kOe)	K_1 (6 K) (erg/cm^3)	$\chi_\perp$ (6 K) (emu/cm^3 Oe)
1 $BaFe_{12}O_{19}$	97.3	67.3	0	0	18.87	4.77×10^6	2.63×10^{-2}
2 $BaFe_{10.2}Sn_{0.74}Co_{0.66}O_{19}$	61.2	55.1	0.620	0.71	~15.97[a]	2.58×10^{6}*	2.03×10^{-2}

[a]H_K was obtained by extrapolating the linear part of $M(H)$ ($H<3$ kOe) to the saturation magnetization M_S (see text).

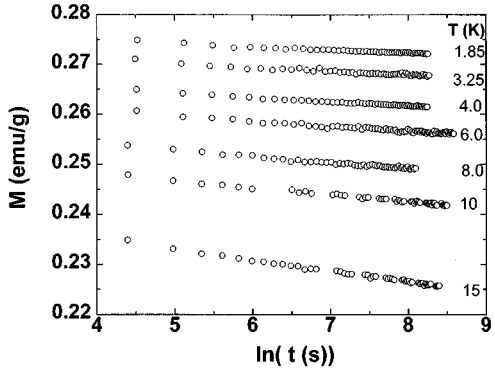

FIG. 3. Remanent magnetization relaxation obtained at different temperatures after field cooled in an external field $H_1=10$ Oe, and applied field in the relaxation measurements $H_2=-220$ Oe.

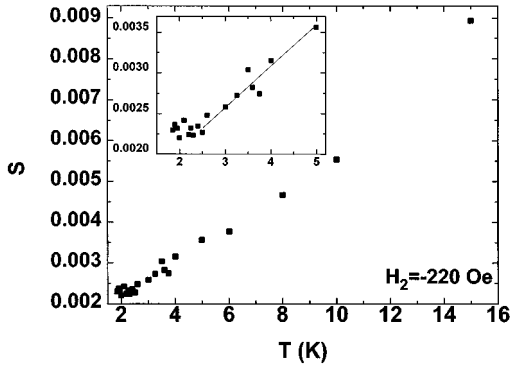

FIG. 4. Magnetic viscosity data as function of temperature; Inset: viscosity curve in the low-temperature regime.

sured during a few hours. Figure 3 shows the relaxation of magnetization obtained at different sample temperatures. The best fitting to these data was given by the logarithmic time dependence of magnetization, indicating that the pinning barriers for the domain-wall motion are not identical, have a distribution of heights. From the fitting, magnetic viscosity $S[S\equiv(1/M_0)dM/d\ \ln\ t]$ can be extracted for different temperatures. The parameter S is a measure of the average energy barrier at a given temperature, and its temperature dependence describes the domain-wall dynamics.

In Fig. 4, we plot the magnetic viscosity, obtained by fitting the data in Fig. 3, as function of temperature. At temperature higher than 3 K, the magnetic viscosity is proportional to temperature, in agreement with the theory of thermally activated decay, which predicts[19] that the viscosity is proportional to temperature at low temperatures (see Fig. 4). As temperature goes to zero, the viscosity S begin to lose the linear dependence on T, and has a temperature-independent tendency, although there are some fluctuations. The temperature-independent tendency of magnetic viscosity below 2.5 K could be the signatures of quantum tunneling of domain walls.

As predicted theoretically by Chudnovsky,[6] the crossover temperature from thermal to the quantum regimes of domain-wall tunneling in antiferromagnets is dominated by the anisotropy constant K and perpendicular susceptibility $\chi_\perp$:

$$k_B T_C \approx \hbar\gamma\sqrt{K/\chi_\perp}, \tag{3}$$

where $\gamma\sim 1.76\times 10^7\ \mathrm{Oe}^{-1}\,\mathrm{s}^{-1}$ is the gyromagnetic ratio. By taking the value of anisotropy constant and perpendicular susceptibility obtained experimentally (in Table I), the calculated crossover temperature, using Eq. (3), gives $T_{c,\mathrm{cal}}\sim 1.5$ K, in qualitative agreement with that obtained experimentally $T_{c,\mathrm{exp}}\sim 2.5$ K (Fig. 4).

In conclusion, we have studied the static properties of a Ba-Fe-Sn-Co-O single crystal. It has been found that substitution of Fe by Sn and Co, reduces the saturation magnetization and produces pinning centers for the domain-wall motion. We have studied the domain-wall motion by relaxation measurements. Above 2.5 K, the depinning of domain walls is due to the thermal activation. Below $T=2.5$ K, it seems that the magnetic viscosity deviates from the linear dependence on temperature, suggesting that the domain-wall motion could be dominated by the quantum mechanism. However, measurements of relaxation at much lower temperature should be carried out to give a clearer evidence of it.

ACKNOWLEDGMENTS

This work was partly supported by the EC project No. CHRX-CT-93-0372 and Ministerio de Educacion y Ciencia, No. MAT94-0320.

[1] E. M. Chudnovsky and L. Gunther, Phys. Rev. Lett. **60**, 661 (1988); Phys. Rev. B **37**, 9455 (1988).

[2] X. X. Zhang, Ll. Balcells, J. M. Ruiz, O. Iglesias, J. Tejada, and B. Barbara, Phys. Lett. A **163**, 130 (1992); X. X. Zhang, Ll. Balcells, J. M. Ruiz, J. L. Tholence, B. Barbara, and J. Tejada, J. Phys. Condens. Matter **4**, L163 (1992); J. Tejada, X. X. Zhang, and C. Ferrarter, Z. Phys. B **94**, 245 (1994); J. Tejada and X. X. Zhang, J. Phys. Condens. Matter **6**, 263 (1994); J. Tejada, X. X. Zhang, Ll. Balcells, O. Iglesias, and B. Barbara, Europhys. Lett. **22**, 211 (1993).

[3] R. H. Kodama, C. L. Seaman, A. E. Berkowitz, and M. B. Maple, J. Appl. Phys. **75**, 5638 (1994).

[4] J. Tejada, X. X. Zhang, and E. M. Chudnovsky, Phys. Rev. B **47**, 14 977 (1993).

[5] J. Tejada, X. X. Zhang, and Ll. Balcells, J. Appl. Phys. **73**, 6709 (1993).

[6] E. M. Chudnovsky, J. Magn. Magn. Mater. **140-144**, 1821 (1995).

[7] J. Tejada and X. X. Zhang, J. Magn. Magn. Mater. **140-144**, 1815 (1995).

[8] B. Barbara *et al.*, J. Appl. Phys. **73**, 6703 (1993); B. Barbara *et al.*, J. Magn. Magn. Mater. **140-144**, 1825 (1995).

[9] P. C. E. Stamp, Phys. Rev. Lett. **66**, 2802 (1991).

[10] B. Barbara and E. M. Chudnovsky, Phys. Lett. A **145**, 205 (1990).

[11] G. Tatara and H. Fukuyama, Phys. Rev. Lett. **72**, 772 (1994), and reference therein.

[12] P. C. E. Stamp, E. M. Chudnovsky, and B. Barbara, Int. J. Mod. Phys. B **6**, 1355 (1992).

[13] X. X. Zhang, J. Tejada, A. Roig, O. Nikolov, and E. Molins, J. Magn. Magn. Mater. **137**, L235 (1994); J. Tejada, X. X. Zhang, A. Roig, O. Nikolov, and E. Molins, Europhys. Lett. **30**, 227 (1995).
[14] L. Néel, Ann. Geophys. **5**, 99 (1949).
[15] W. F. Brown, Phys. Rev. **130**, 1677 (1963).
[16] R. A. Schippan and K. A. Hempel, J. Magn. Magn. Mater. **38**, (319) 1983; Y. S. Shur and V. I. Khrabrov, Sov. Phys. JETP. **30**, 1027 (1970).
[17] F. Sandiumenge, B. Martinez, X. Batlle, S. Galí, and X. Obradors, J. Appl. Phys. **72**, 4608 (1992).
[18] Yu. G. Chukalkin, V. V. Petrov, and B. N. Goshchtskii, Phys. Status Solidi A **67**, 421 (1981).
[19] R. Street and J. C. Woolley, Proc. Phys. Soc. London Ser. A **62**, 562 (1949); L. Néel, J. Phys. (Paris) **11**, 49 (1950).